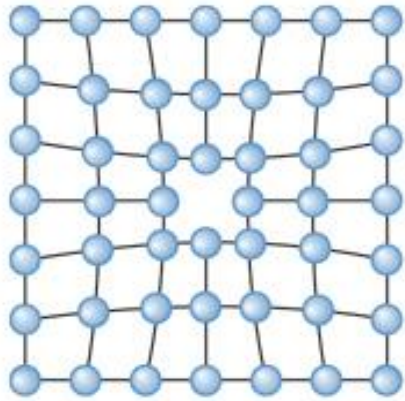




# Defeitos

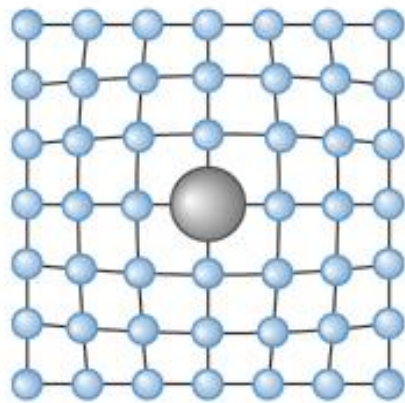


(a)

Explicar equilíbrio de vacâncias. Mostrar exemplo do Cu ( $Q_v=20$  kcal/mol).

$$n_v = N \exp\left(\frac{-Q_v}{RT}\right)$$

**Figure 4.1 Point defects: (a) vacancy.**  
All of these defects disrupt the perfect arrangement of the surrounding atoms.



(d)

**Figure 4.1 Point defects: (d) large substitutional atom. All of these defects disrupt the perfect arrangement of the surrounding atoms.**

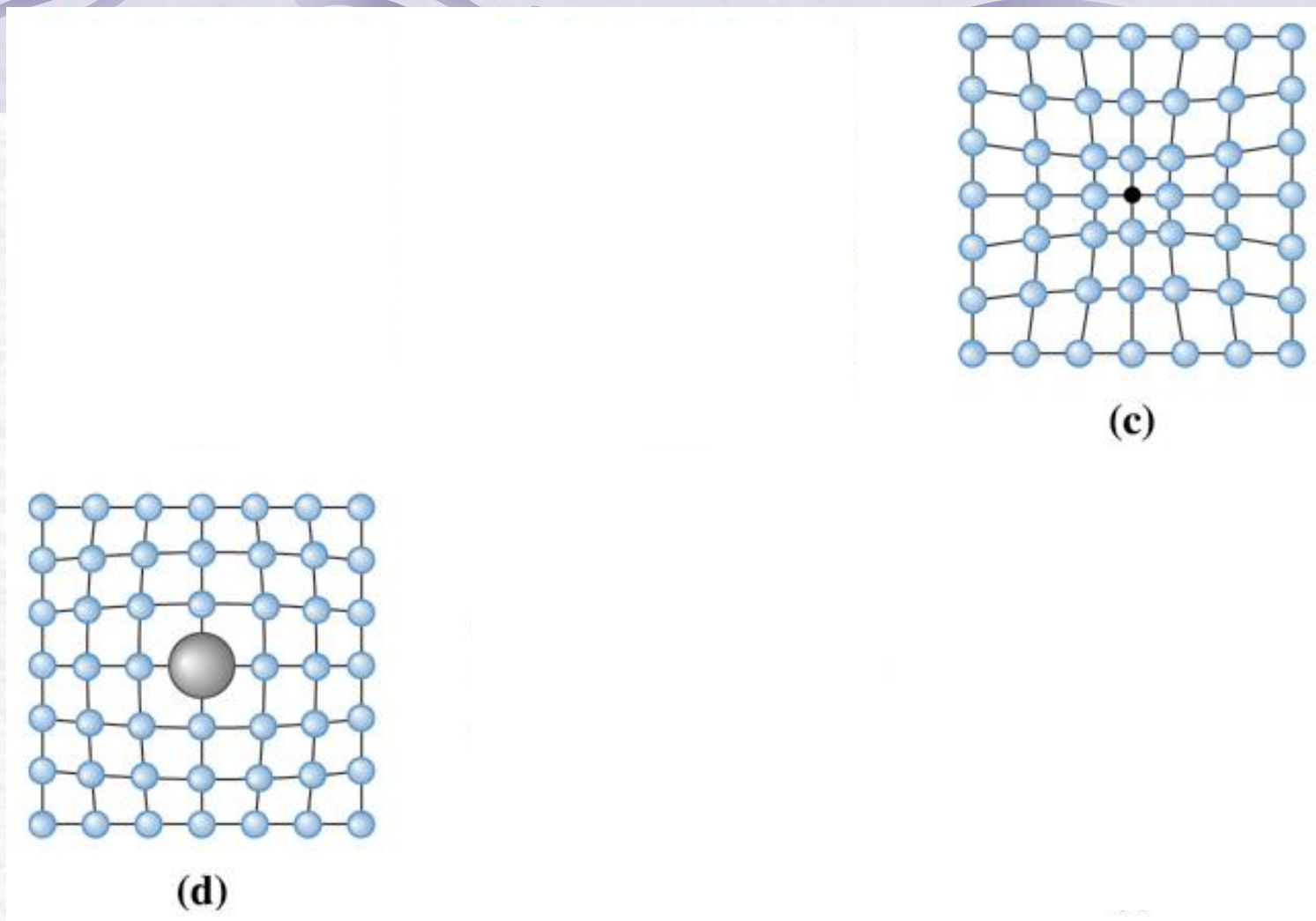
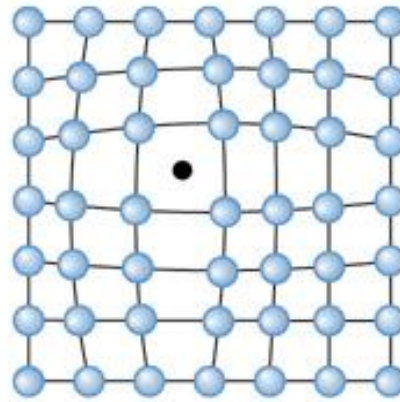


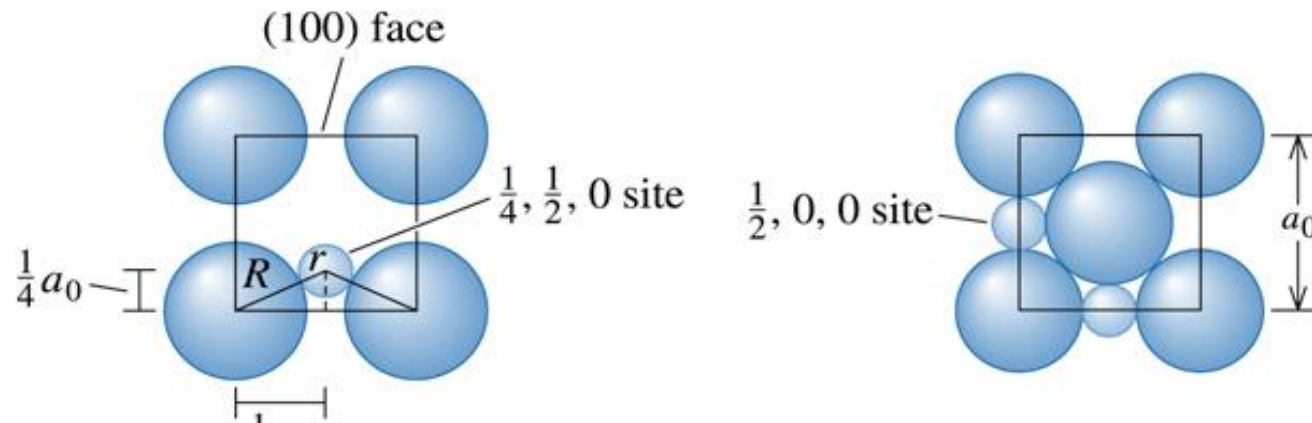
**Figure 4.1 Point defects: (c) small substitutional atom, (d) large substitutional atom. All of these defects disrupt the perfect arrangement of the surrounding atoms.**



(b)

**Figure 4.1 Point defects: (b) interstitial atom.**  
All of these defects disrupt the perfect arrangement of the surrounding atoms.





Explicar : Fase, Solução Sólida e regra de Hume-Rothery.

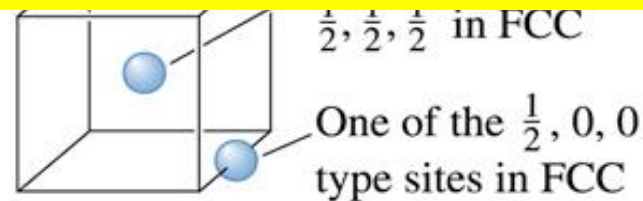


**Figure 4.2 (a) The location of the  $\frac{1}{4}, \frac{1}{2}, 0$  interstitial site in BCC metals, showing the arrangement of the normal atoms and the interstitial atom (b)  $\frac{1}{2}, 0, 0$  site in FCC metals, (for Example 4.3). (c) Edge centers and cube centers are some of the interstitial sites in the FCC structure (Example 4.3).**

# Discordância em cunha

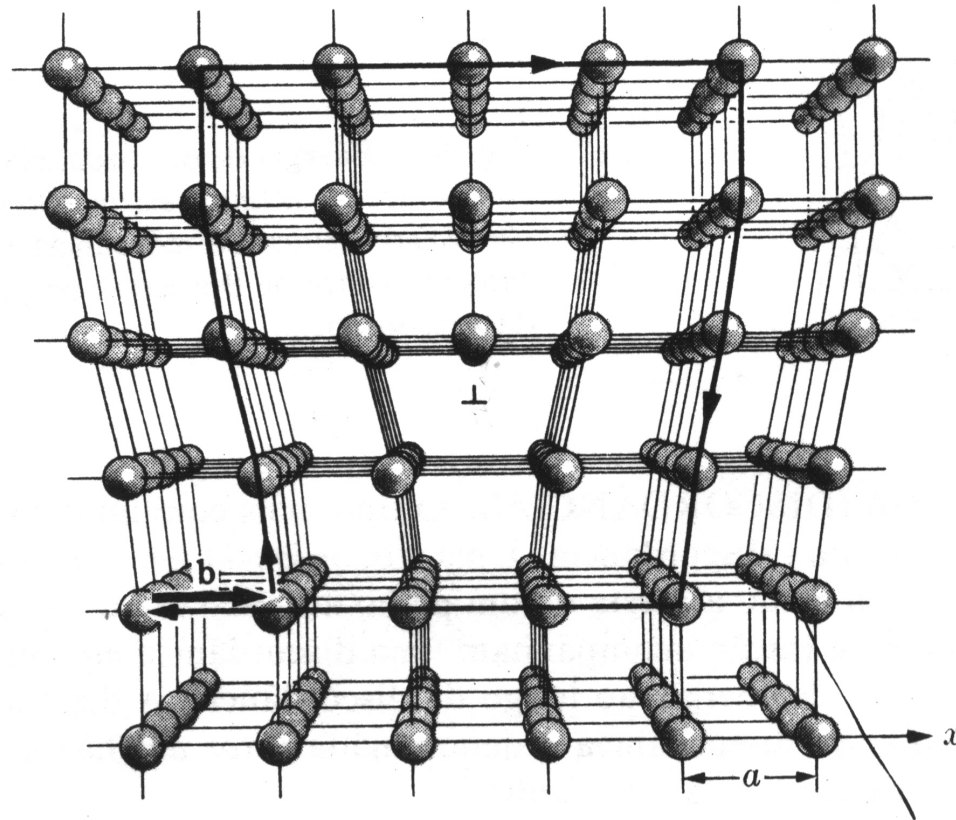
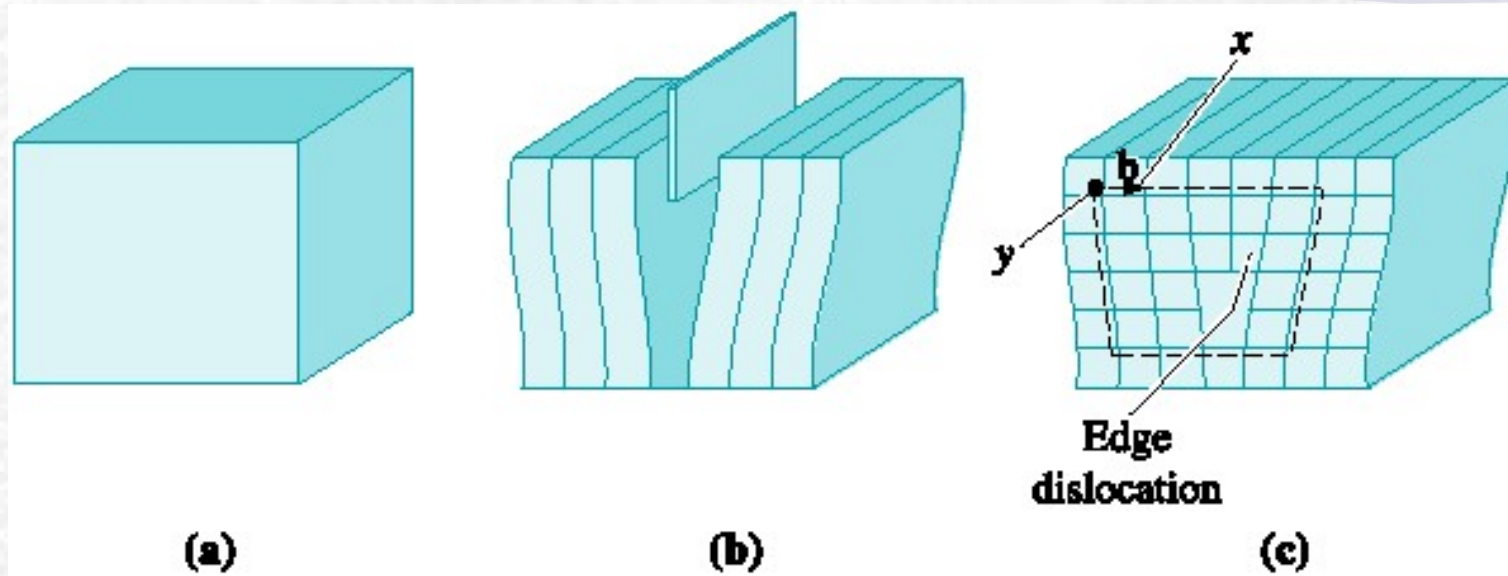


Fig. 4-10. Discordância em cunha. Um defeito de linha ocorre na aresta de um plano atômico extra. (Guy, A. G., *Elements of Physical Metallurgy*, Reading, Mass.: Addison Wesley, 1959, pág. 110).

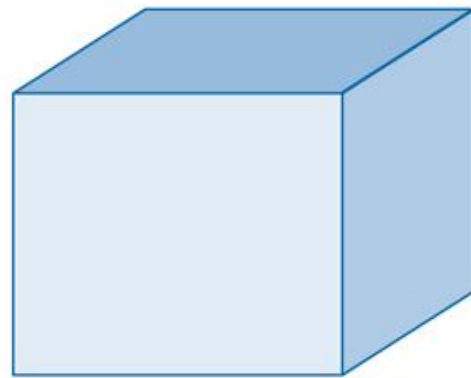


**Figure 4.5** The perfect crystal in (a) is cut and an extra plane of atoms is inserted (b). The bottom edge of the extra plane is an edge dislocation (c). A Burgers vector  $b$  is required to close a loop of equal atom spacings around the edge dislocation. (*Adapted from J.D. Verhoeven, Fundamentals of Physical Metallurgy, Wiley, 1975.*)

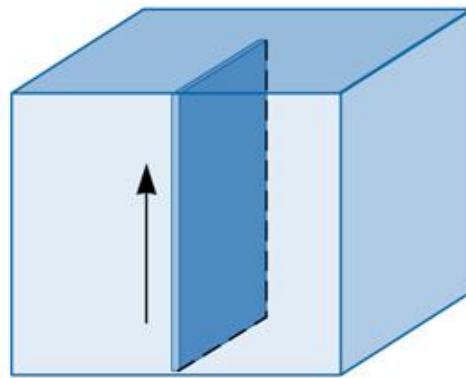


# Discordância em hélice

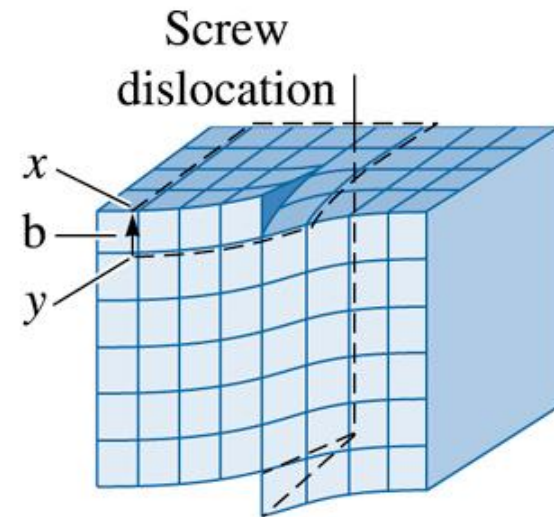
(c) 2003 Brooks/Cole Publishing / Thomson Learning



(a)



(b)



(c)

**Figure 4.4** the perfect crystal (a) is cut and sheared one atom spacing, (b) and (c). The line along which shearing occurs is a screw dislocation. A Burgers vector  $b$  is required to close a loop of equal atom spacings around the screw dislocation.

# Discordância em hélice

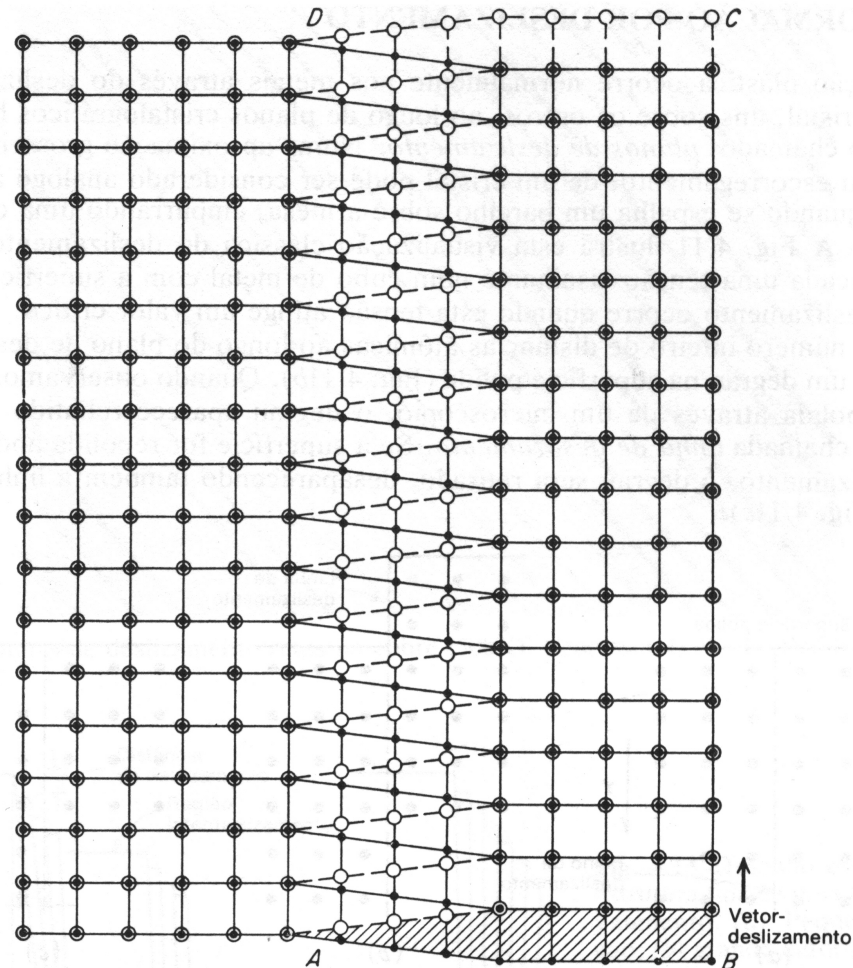
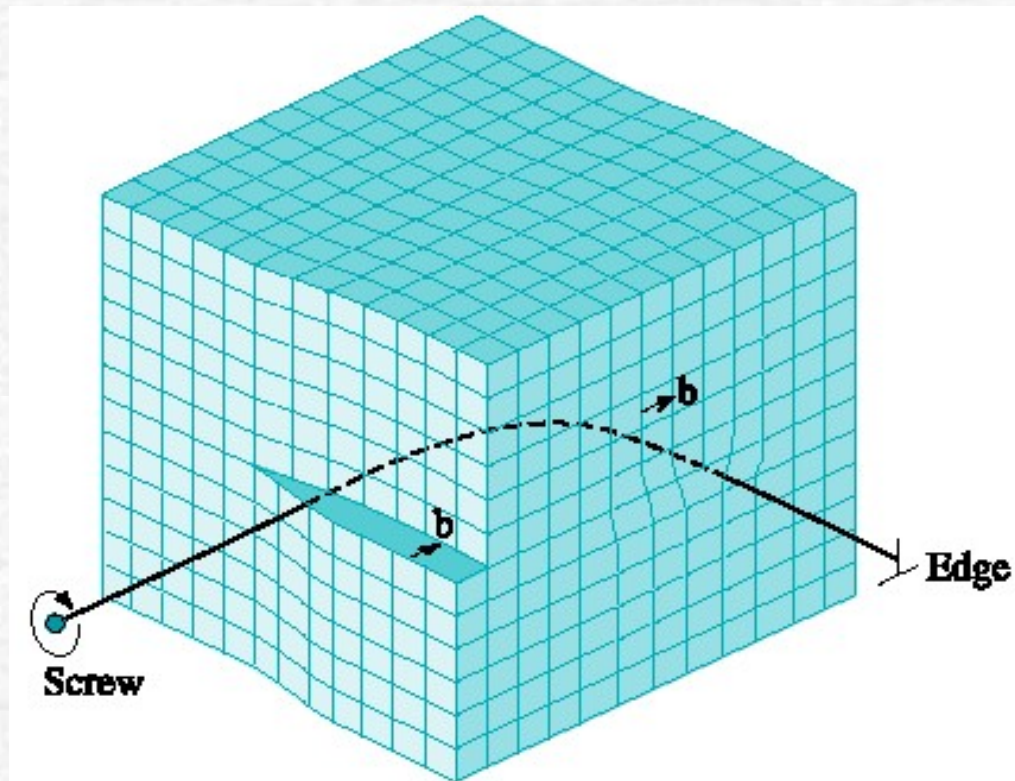


**Fig. 4.10** Arranjo atômico em volta da discordância espiral mostrada na Fig. 4.9. O plano da figura é paralelo ao plano de deslizamento. A área deslocada é  $ABCD$ , e  $AD$  é a discordância-espiral. Os círculos abertos representam os átomos imediatamente acima do plano de deslizamento; os círculos fechados são os átomos no plano imediatamente abaixo do plano de deslizamento. (De W. T. Read, Jr., *Dislocations in Crystals*, p. 17, McGraw-Hill Book Company, New York, 1953.)

# Mista



*McGraw-Hill, 1953.)*



# Discordâncias

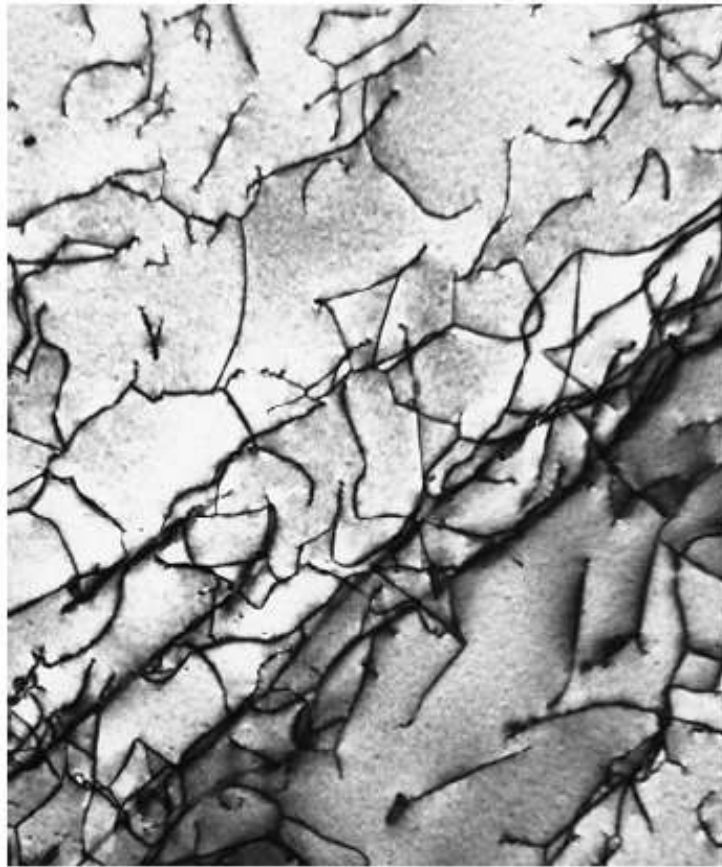


**Figure 4.6** A transmission electron micrograph of a titanium alloy in which the dark lines are dislocations. 51,450 $\times$ . (Courtesy of M. R. Plichta, Michigan Technological University.)



# Vetor de Burgers

A sketch of a dislocation in magnesium oxide (MgO), which has the sodium chloride crystal structure and a lattice parameter of 0.396 nm, is shown in Figure 4.9. Determine the length of the Burgers vector.

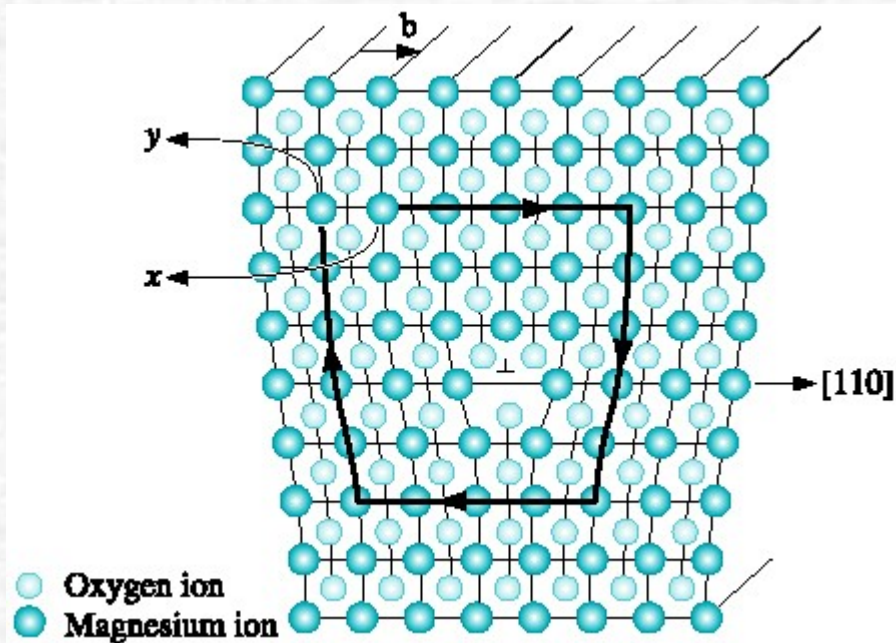


**Figure 4.9** An edge dislocation in MgO showing the slip direction and Burgers vector (for Example 4.7). (Adapted from W.D. Kingery, H.K. Bowen, and D.R. Uhlmann, *Introduction to Ceramics*, John Wiley, 1976.) for Example 4.7)

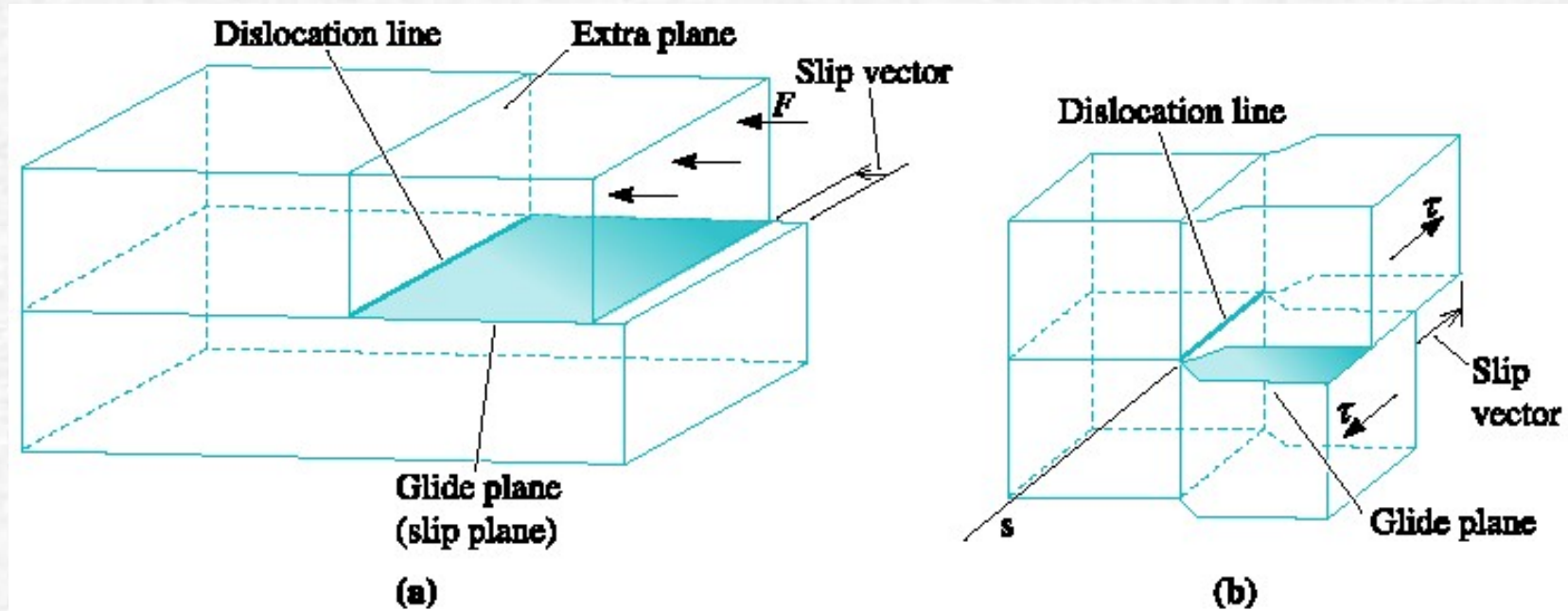


**Figure 4.7 Schematic of slip line, slip plane, and slip (Burgers) vector for (a) an edge dislocation and (b) for a screw dislocation. (Adapted from J.D. Verhoeven, Fundamentals of Physical Metallurgy, Wiley, 1975.)**

**TABLE 4-1 ■ Slip planes and directions in metallic structures**

Crystal Structure	Slip Plane	Slip Direction
BCC metals	{110} {112} {123}	$\langle 111 \rangle$
FCC metals	{111}	$\langle 110 \rangle$
HCP metals	{0001}	$\langle 100 \rangle$
	{11 $\bar{2}$ 0}	$\langle 110 \rangle$
	{10 $\bar{1}$ 0}	or $\langle 11\bar{2}0 \rangle$
	{10 $\bar{1}$ 1}	
MgO, NaCl (ionic)	{110}	$\langle 110 \rangle$
Silicon (covalent)	{111}	$\langle 110 \rangle$

*Note: These planes are active in some metals and alloys or at elevated temperatures.*

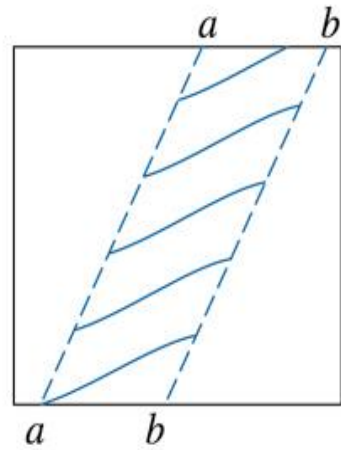
**TABLE 4-2** ■ *Summary of factors affecting slip in metallic structures*

<b>Factor</b>	<b>FCC</b>	<b>BCC</b>	<b>HCP <math>\left(\frac{c}{a} &gt; 1.633\right)</math></b>
Critical resolved shear stress (psi)	50–100	5,000–10,000	50–100 <sup>a</sup>
Number of slip systems	12	48	3 <sup>b</sup>
Cross-slip	Can occur	Can occur	Cannot occur <sup>b</sup>
Summary of properties	Ductile	Strong	Relatively brittle

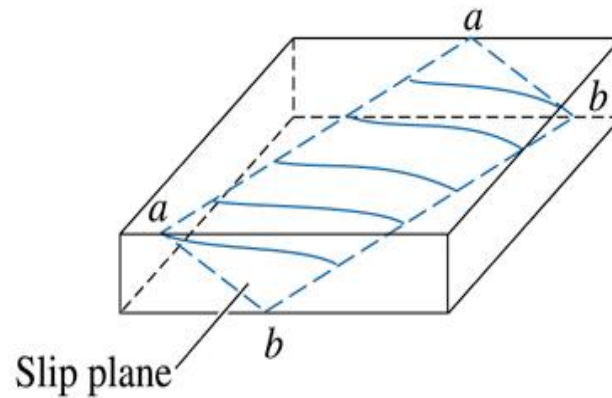
<sup>a</sup> For slip on basal planes.

<sup>b</sup> By alloying or heating to elevated temperatures, additional slip systems are active in HCP metals, permitting cross-slip to occur and thereby improving ductility.

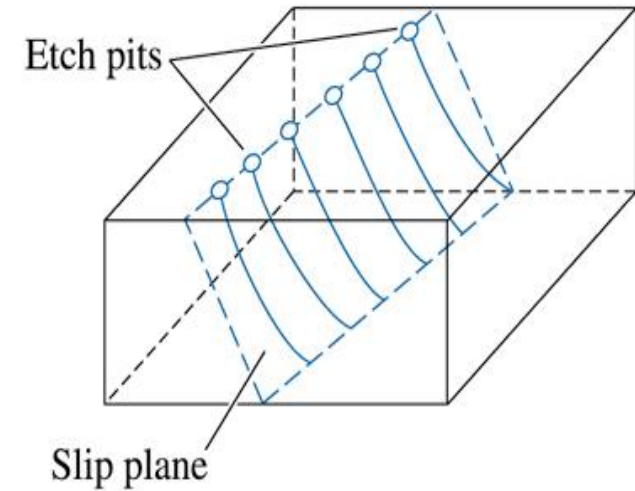




(a)



(b)



(c)

**Figure 4.11** A sketch illustrating dislocations, slip planes, and etch pit locations. (Source: Adapted from *Physical Metallurgy Principles, Third Edition*, by R.E. Reed-Hill and R. Abbaschian, p. 92, Figs. 4-7 and 4-8. Copyright (c) 1992 Brooks/Cole Thomson Learning. Adapted by permission.)

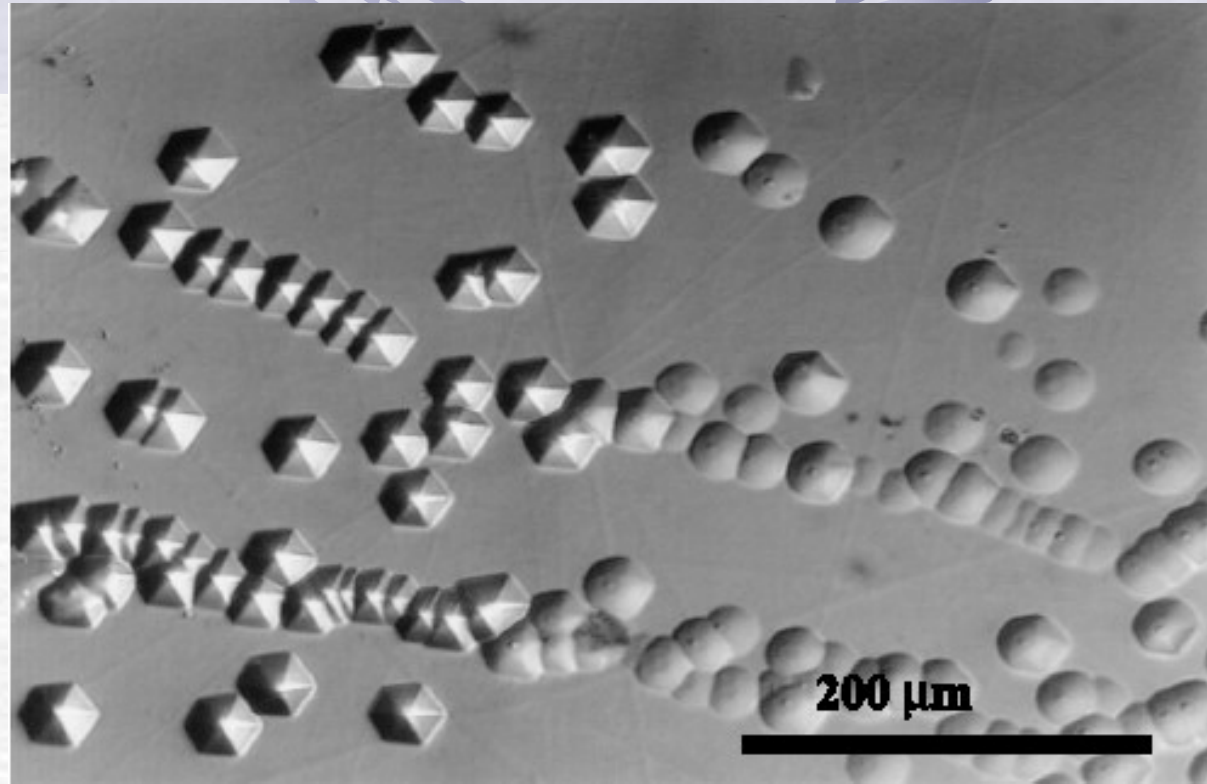


**Figure 4.12** Optical image of etch pits in silicon carbide (SiC). The etch pits correspond to intersection points of pure edge dislocations with Burgers vector  $a/3 \langle 1120 \rangle$  and the dislocation line direction along  $[0001]$  (perpendicular to the etched surface). Lines of etch pits represent low angle grain boundaries (*Courtesy of Dr. Marek Skowronski, Carnegie Mellon University.*)

# Interfaces

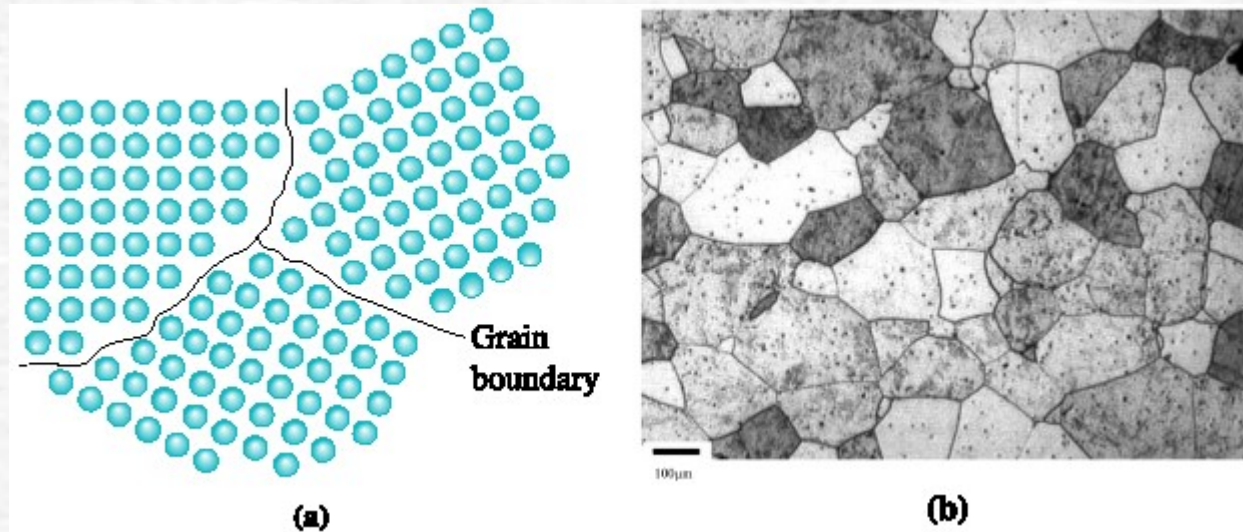


**Figure 4.16 (a) The atoms near the boundaries of the three grains do not have an equilibrium spacing or arrangement. (b) Grains and grain boundaries in a stainless steel sample. (Courtesy Dr. A. Deardo.)**



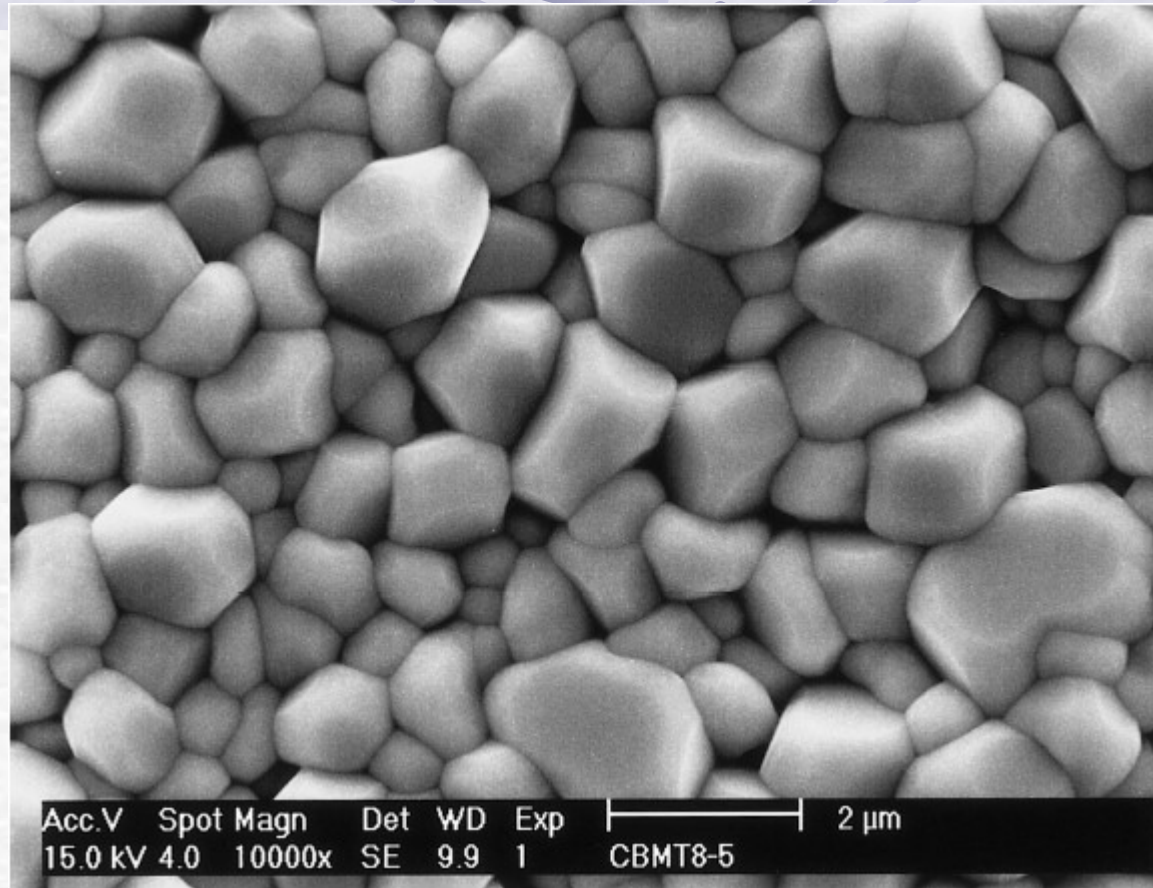


**Figure 4.24** The microstructure of BMT ceramics obtained by compaction and sintering of BMT powders. (*Courtesy of H. Shirey.*)



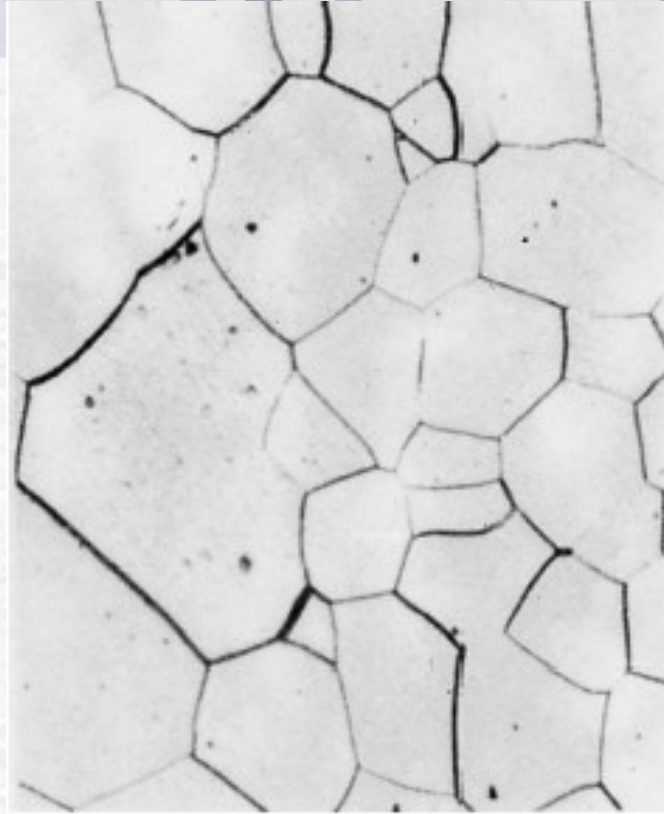
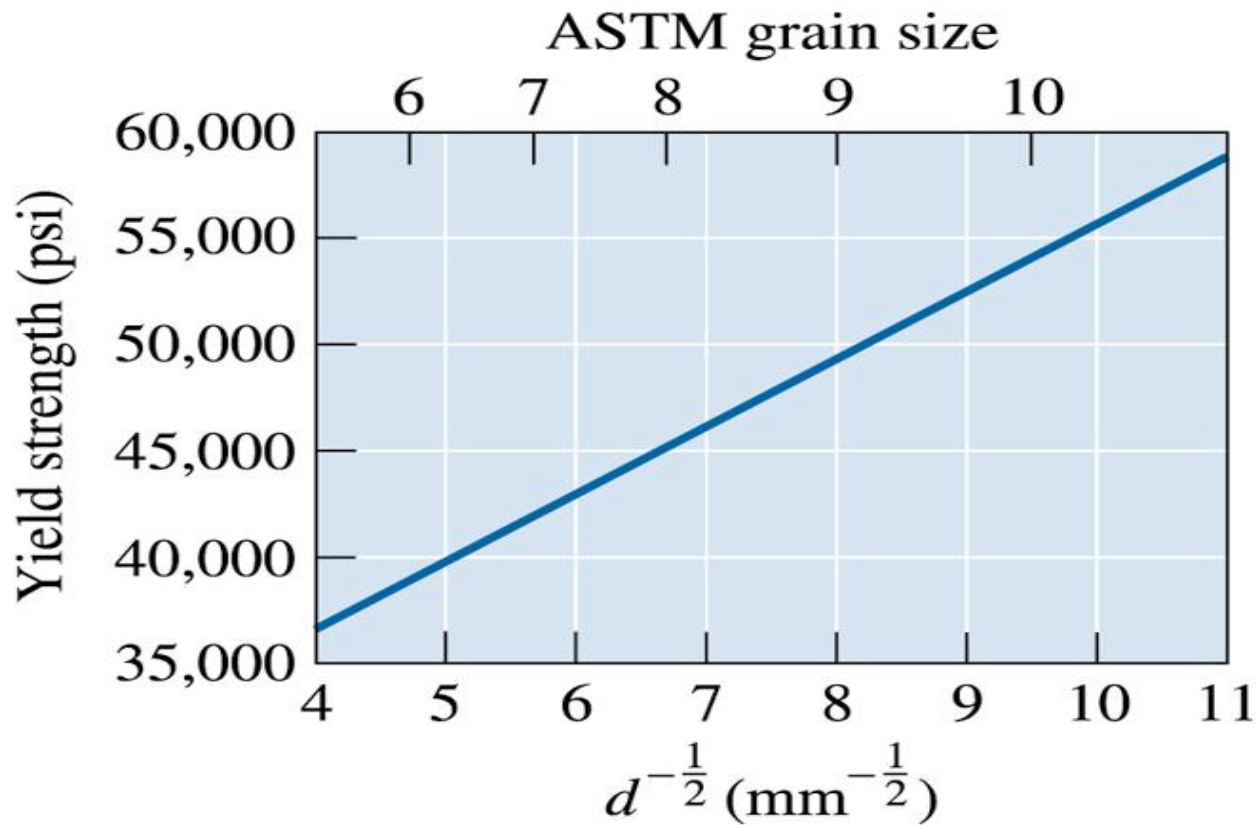


**Figure 4.18 Microstructure of palladium (x 100). (From ASM Handbook, Vol. 9, Metallography and Microstructure (1985), ASM International, Materials Park, OH 44073.)**

Lembrar de Hall-Petch



(c) 2003 Brooks/Cole Publishing / Thomson Learning

**Figure 4.17** The effect of grain size on the yield strength of steel at room temperature.

$$H = H_0 + k_H d^{-1/2}$$

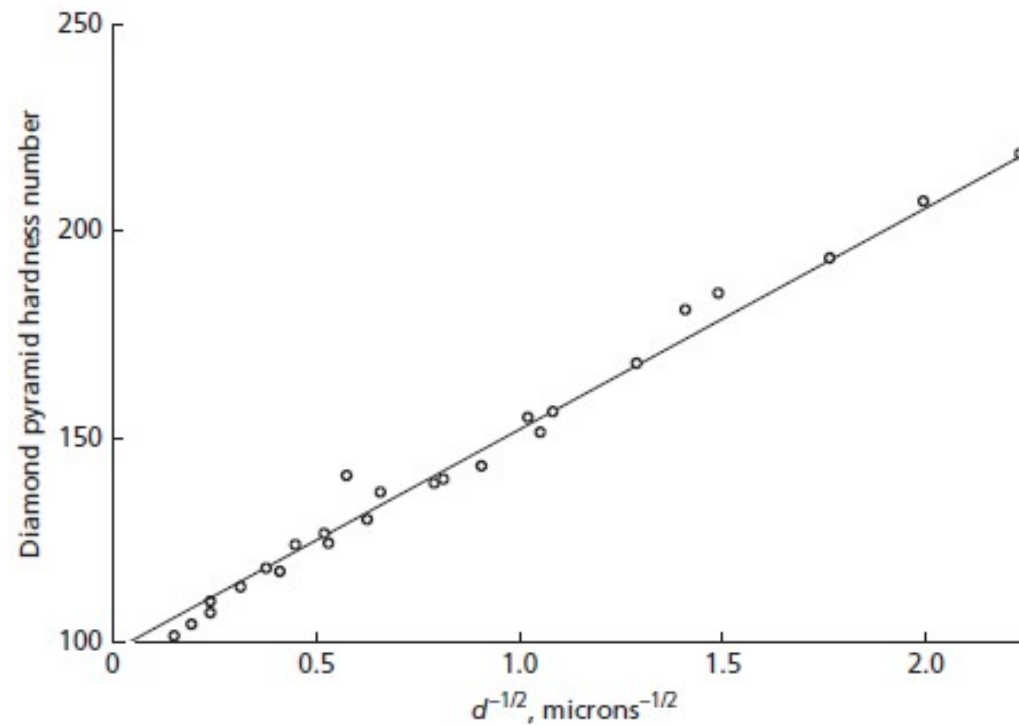


**FIG. 6.23** The hardness of titanium as a function of the reciprocal of the square root of the grain size. (From the data of H. Hu and R. S. Cline, *TMS-AIME*, 242 1013 [1968]. This data has been previously presented in this form by R. W. Armstrong and P. C. Jindal, *TMS-AIME*, 242 2513 [1968].)

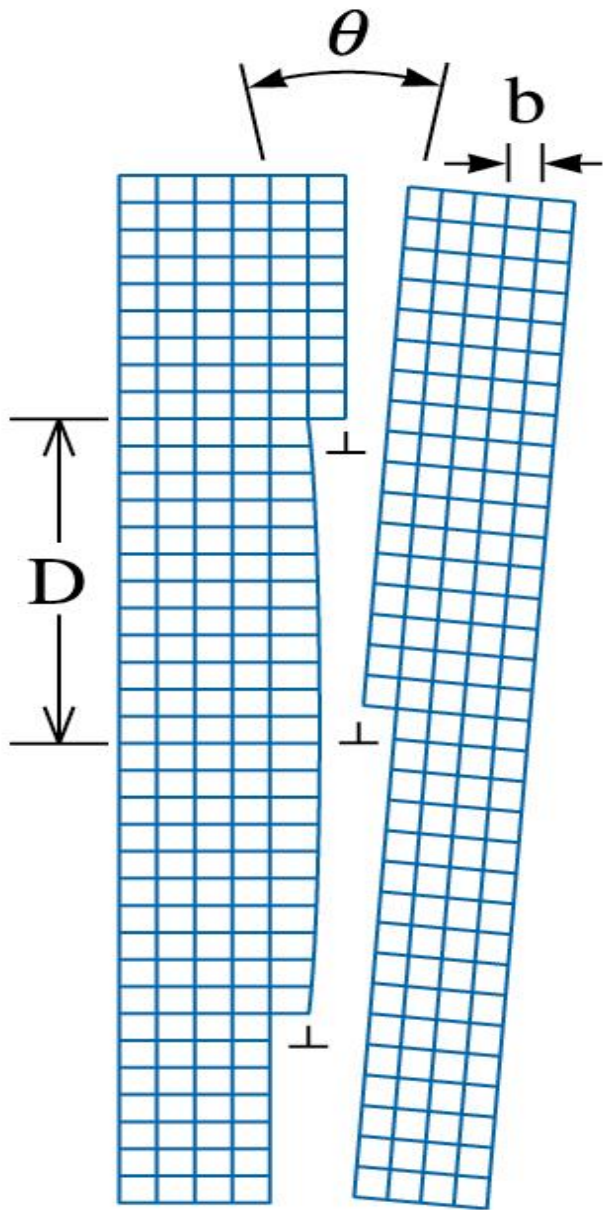
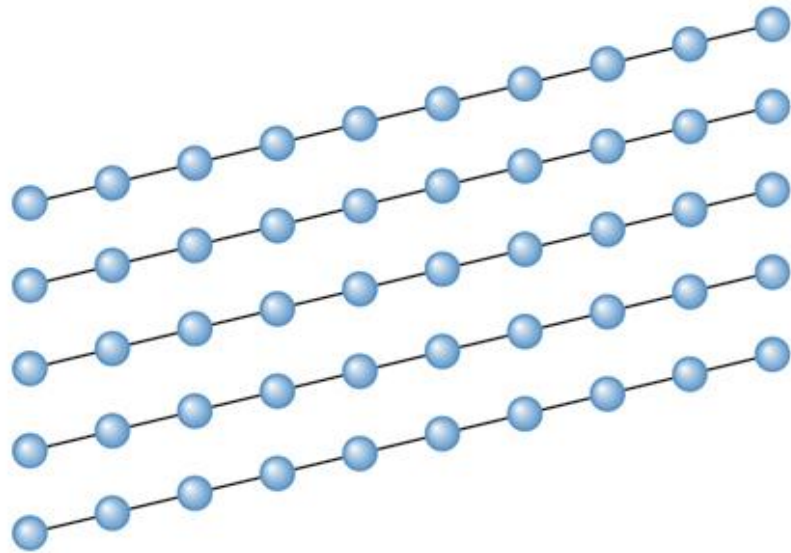
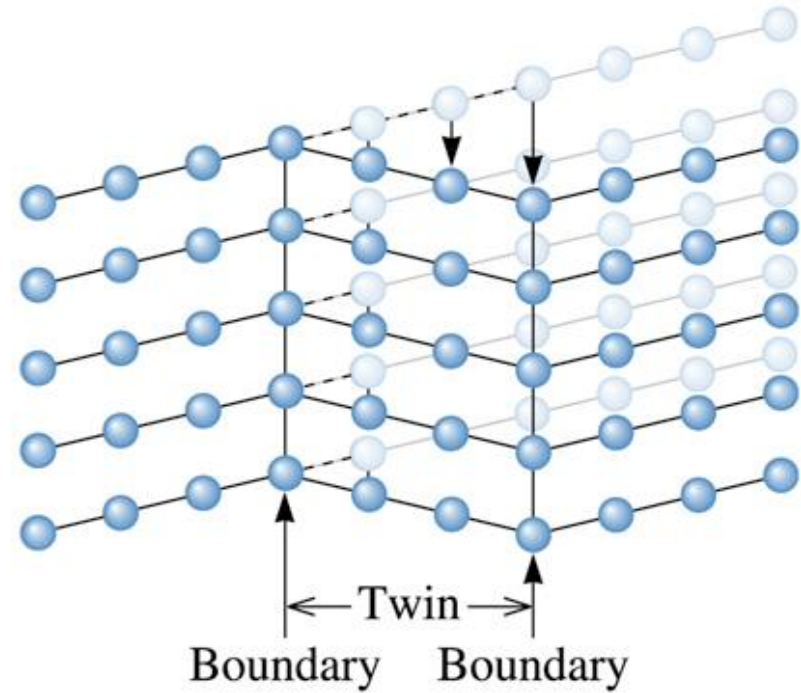


**Figure 4.19** The small angle grain boundary is produced by an array of dislocations, causing an angular mismatch  $\theta$  between lattices on either side of the boundary.



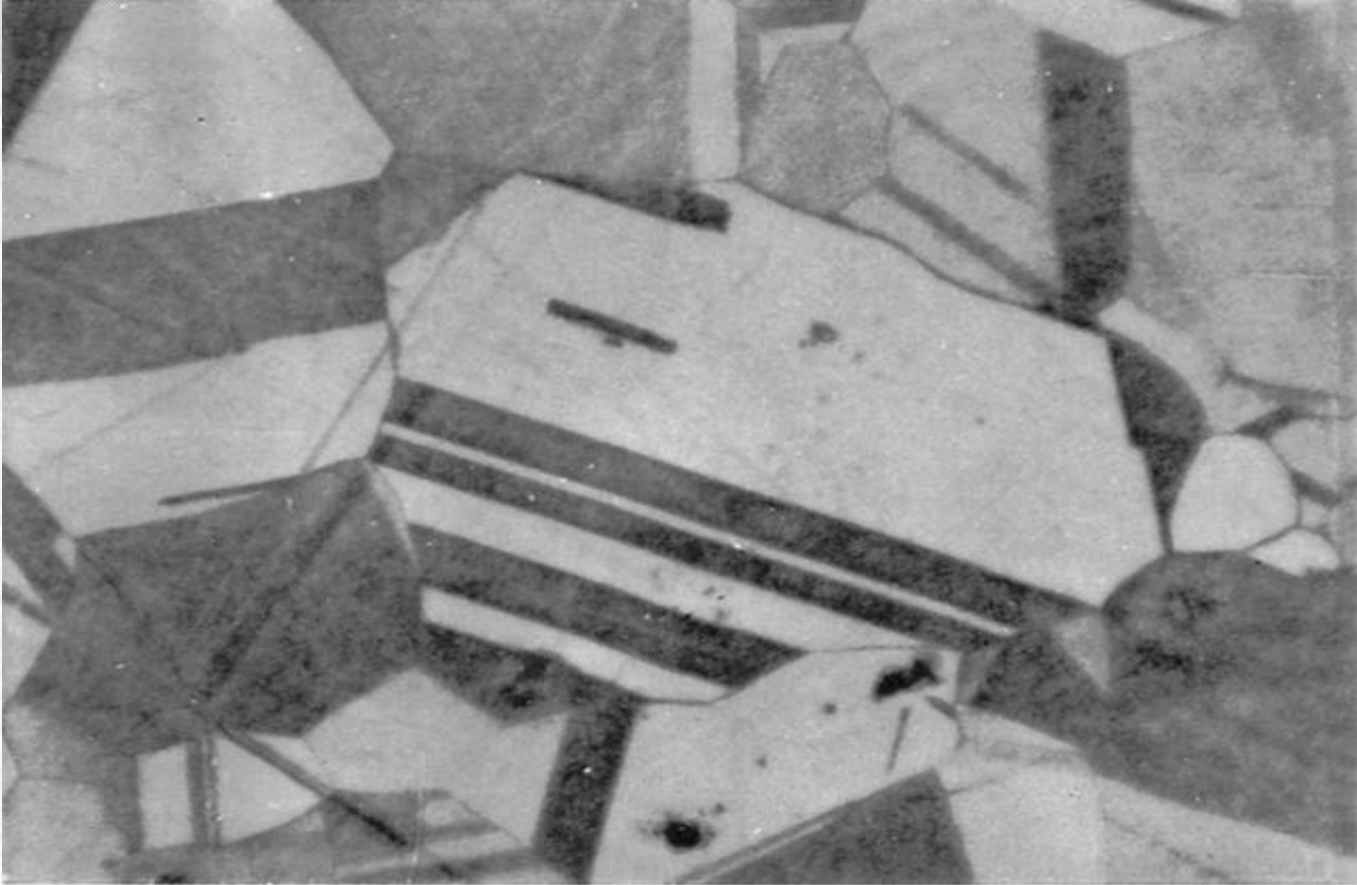


(a)



(b)

**Figure 4.20 Application of a stress to the perfect crystal (a) may cause a displacement of the atoms, (b) causing the formation of a twin. Note that the crystal has deformed as a result of twinning.**



(c)

**Figure 4.20 (c) A micrograph of twins within a grain of brass (x250).**

**TABLE 4-3** ■ *Energies of surface imperfections in selected metals*

<b>Surface Imperfection (energy/cm<sup>2</sup>)</b>	<b>Al</b>	<b>Cu</b>	<b>Pt</b>	<b>Fe</b>
Stacking fault	200	75	95	—
Twin boundary	120	45	195	190
Grain boundary	625	645	1000	780

Explicar falha de empilhamento

# Defeitos de volume

## ▮ microestruturais

- poros
- trincas
- inclusões